



國立臺灣大學
National Taiwan University

Looking for deviations in the large scale structure

Fabien Nugier

LeCosPA

National Taiwan University

CosPA 2017

13th December, 2017

Yukawa Institute for Theoretical Physics

Kyoto University, Japan

The large scale structure

(Very) tentative definition :

"Everything above galaxy scale that is sensitive to gravitational instability."

2dFGRS (2002) :

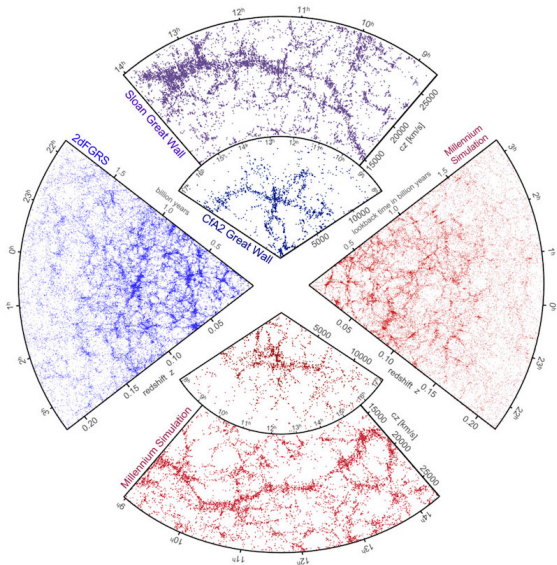
- 2.5 Gly depth on 2 slices
- ~ 1500 sqdeg area
- spectra for ~ 250k objects
- <http://www.2dfgrs.net/>

Millennium Run (2005) :

- 10 G particles
- 2 Gly box
- ~ 20 M galaxies

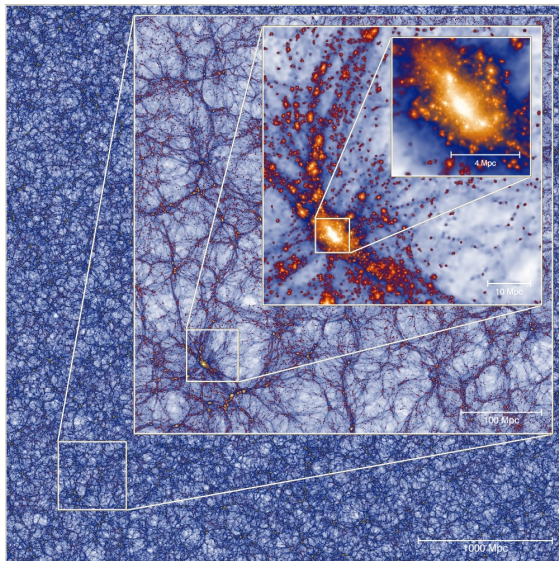
Sloan Digital Sky Survey :

- 3 M spectra
- ~ 35% of the sky



Millennium-XXL (2010)

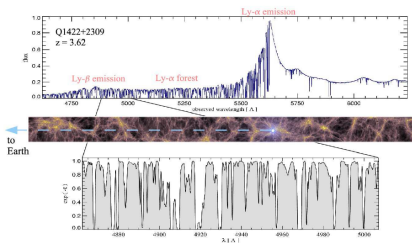
- 300 billion particles
whole Univ. to $z \sim 0.72$
- goal 1 : relation between optical richness, lensing mass, X-ray luminosity and thermal Sunyaev-Zeldovich (tSZ) signal from CMB
- goal 2 : mass of extreme galaxy clusters
- **useful for other probes :**
BAOs, redshift space distortions (RSD), cluster number counts, weak gravitational lensing (WL), integrated Sachs-Wolfe (ISW) effect.
- halo mass function, power spectrum
- gives optical, lensing, X-ray, tSZ maps, galaxy clusters catalogues



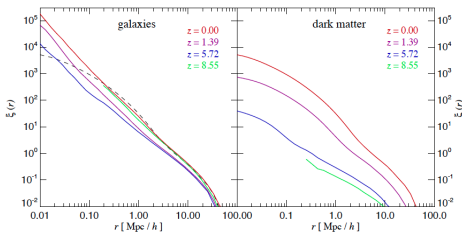
See [Angulo et al. 2013](#).

Examples of probes

- Intergalactic H absorption lines in quasar spectra \Rightarrow Lyman- α forest.



- 2pt-correl. (of galaxies or DM) \Leftrightarrow Power spectrum $P_g(\mathbf{k}) = b^2 P_m(\mathbf{k})$



Two aspects of this talk

- **RELATIVISTIC CORRECTIONS DUE TO THE LSS :**
how does the LSS affects cosmological observables, how we can use adapted coordinates which actually simplify calculations.



- **COMPARING STANDARD CANDLES AND GALAXY CATALOGUES IN OUR LOCAL UNIVERSE :**
what can we learn by comparing these probes, what it can say about the H_0 tension, supernovae or galaxy catalogues.



PART I

RELATIVISTIC CORRECTIONS DUE TO THE LSS

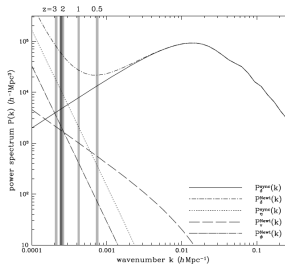


Relativistic corrections to LSS

Context : Perturbations around a FLRW background.

Galaxy clustering (Yoo, Fitzpatrick, Zaldarriaga '09, Yoo '10) :

- $\delta_g = b \delta_m$ is affected by relativistic corrections.
- δ_m and $b(k)$ are both **gauge dependent** quantities.
- gauge effects appear near horizon and at large z (where Newt. approx. is not valid) \Rightarrow **Test of GR!**
- total number of observed galaxies is affected by matter perturbations.

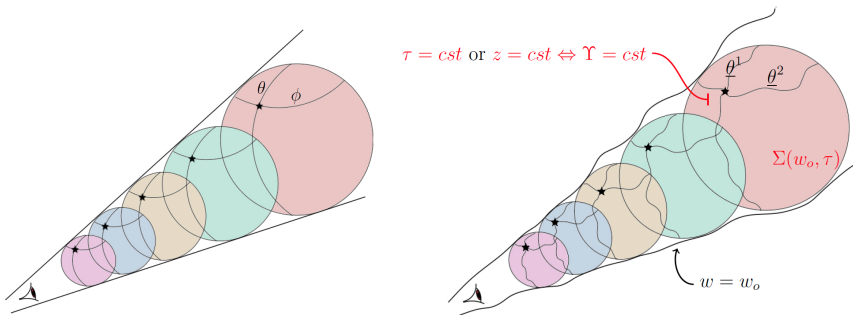


Generalization of **Kaiser formula** (valid at small scales) relating redshift-space power spectrum $P_s(\mathbf{k}, \mu_k)$ and $P_m(\mathbf{k})$ (Montanari, Durrer '12, Bertacca *et al.*'12, Yoo, Seljak '13).

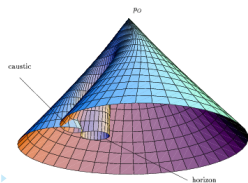
Impact of relativistic corrections : luminosity distance (Hubble diagram), redshift, angles (gravitational lensing), volumes (number counts).

Geodesic Light Cone coordinates (GLC)

Adapted coordinates : Simplify relativistic calculations by working in coordinates defined from observable (gauge-invariant) quantities.



History : Temple 1938, Joseph '58, Saunders '68, Maartens '84, Gasperini, Marozzi, N., Veneziano 2011.



$$ds_{\text{GLC}}^2 = \Upsilon^2 dw^2 - 2\Upsilon dw d\tau + \gamma_{ab} (d\underline{\theta}^a - U^a dw)(d\underline{\theta}^b - U^b dw)$$

(6 arbitrary functions : $\Upsilon, U^a, \gamma_{ab}$)

w is a **null coordinate**, $\partial_\mu \tau$ defines a **geodesic flow** (from $g_{\text{GLC}}^{\tau\tau} = -1$),
 photons travel at $(w, \underline{\theta}^a) = \overrightarrow{cst} \perp$ to $\Sigma(w, z)$.

Υ is like an **inhomogeneous scale factor** (lapse function), U^a is a **shift-vector** and γ_{ab} the **metric inside the 2-sphere** $\Sigma(\tau, w)$.

$$\begin{aligned} \text{FLRW : } w &= \eta + r, \quad \tau = t, \quad (\underline{\theta}^1, \underline{\theta}^2) = (\theta, \phi), \\ \Upsilon &= a(t), \quad U^a = 0, \quad \gamma_{ab} = a^2 r^2 \text{diag}(1, \sin^2 \theta). \end{aligned}$$

Residual gauge freedoms : relabeling light cones/rays; reparametrizing light rays; conformal transformations (Fleury, N., Fanizza '16, Scaccabarozzi, Yoo '17)

⇒ **Redshift perturbation** :

$$(1 + z_s) = \frac{(k^\mu u_\mu)_s}{(k^\mu u_\mu)_o} = \frac{(\partial^\mu w \partial_\mu \tau)_s}{(\partial^\mu w \partial_\mu \tau)_o} = \frac{\Upsilon(w_o, \tau_o, \underline{\theta}^a)}{\Upsilon(w_o, \tau_s, \underline{\theta}^a)} \equiv \frac{\Upsilon_o}{\Upsilon_s}$$

where $u_\mu = -\partial_\mu \tau$ is the **peculiar velocity** of the **comoving** observer/source and $k_\mu = \partial_\mu w$ is the **photon momentum**.

⇒ **(exact) Angular distance** (with homogeneous observer neighborhood) :

$$d_A = \gamma^{1/4} (\sin \underline{\theta}^1)^{-1/2} \quad \text{with} \quad \gamma \equiv \det(\gamma_{ab}) = |\det(g_{\text{GLC}})| / \Upsilon^2$$

which, combined with redshift, gives the **distance-redshift relation**.

⇒ expressions of **luminosity distance** $d_L = (1 + z)^2 d_A$ and **distance modulus** $\mu = 5 \log_{10}(d_L) + \text{cst.}$

Distance-redshift relation at $\mathcal{O}(2)$

- Define scalar perturbations in the Newtonian gauge :

$$ds_{NG}^2 = a^2(\eta) \left(-(1 + 2\Phi)d\eta^2 + (1 - 2\Psi)(dr^2 + \gamma_{ab}^{(0)}d\theta^a d\theta^b) \right)$$

with $\gamma_{ab}^{(0)} = r^2 \text{diag}(1, \sin^2 \theta)$, $\Phi = \psi + \frac{1}{2}\phi^{(2)}$, $\Psi = \psi + \frac{1}{2}\psi^{(2)}$, and taking $\psi^{(2)}, \phi^{(2)} \propto \nabla^{-2}(\partial_i \psi \partial^i \psi)$, $\partial_i \psi \partial^i \psi$ (cf. Bartolo, Matarrese, Riotto, 2005)

- Establish transformation between GLC and NG at second order in PT :

$$(\tau, w, \tilde{\theta}^1, \tilde{\theta}^2) = f(\eta, r, \theta, \phi) \Rightarrow (\Upsilon, U^a, \gamma^{ab}) = f(\psi, \psi^{(2)}, \phi^{(2)})$$

- Use $d_L = (1+z)^2 d_A = (1+z)^2 \gamma^{1/4} \left(\sin \tilde{\theta}^1 \right)^{-1/2}$ up to $\mathcal{O}(2)$ to get :

$$d_L(z_s, \underline{\theta}^a) = d_L^{FLRW}(z_s) \left(1 + \delta_S^{(1)}(z_s, \underline{\theta}^a) + \delta_S^{(2)}(z_s, \underline{\theta}^a) \right)$$

- Details in 1104.1167, 1209.4326, 1506.02003, contributors : Ben-Dayan, Fanizza, Gasperini, Marozzi, N., Veneziano, in qualitative agreement with Umeh, Clarkson and Maarten '14, Bonvin, Clarkson, Durrer, Maartens, Umeh '15, Kaiser, Peacock '15, and recently Yoo, Scaccabarozzi '16!

At $\mathcal{O}(1)$:

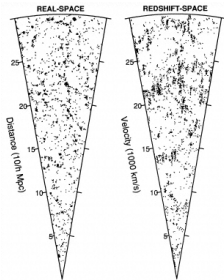
$$\delta_S^{(1)}(z_s, \theta^a) \sim \text{SW} + \text{ISW} + \text{Doppler} - \left(\psi_s^{(1)} + \int_{\eta_+}^{\eta_-} dx \psi \right) - \text{Lensing}^{(1)}$$

$$\text{Lensing}^{(1)} = \frac{1}{2} \nabla_a \theta^{a(1)} = \int_{\eta_s^{(0)}}^{\eta_o} \frac{d\eta}{\Delta\eta} \frac{\eta - \eta_s^{(0)}}{\eta_o - \eta} \Delta_2 \psi(\eta, \eta_o - \eta, \bar{\theta}^a)$$

$$\text{Doppler} = \left(1 - \frac{1}{\mathcal{H}_s \Delta\eta} \right) (\mathbf{v}_o - \mathbf{v}_s) \cdot \hat{n} \quad , \quad \mathbf{v} \equiv \int_{\eta_{in}}^{\eta} d\eta' \frac{a(\eta')}{a(\eta)} \nabla \psi(\eta', r, \theta^a)$$

At $\mathcal{O}(2)$, full calculation :

- Dominant terms : (Doppler)², (Lensing)²!!!
- Combinations of $\mathcal{O}(1)$ -terms : ψ_s^2 , ([ISW])², [ISW] × Doppler, $(\psi_s, \int_{\eta_+}^{\eta_-} dx \psi) \times$ (Lensing, [ISW], Doppler) ...
- Genuine $\mathcal{O}(2)$ -terms : $\psi_s^{(2)}$, $\text{Lensing}^{(2)} = \frac{1}{2} \nabla_a \theta^{a(2)}$, $Q_s^{(2)}$...
- A LOT of other contributions : New integrated effects, Angle deformations, Redshift perturbations (⊂ transverse peculiar velocity), Lens-Lens coupling, corrections to Born approximation, ... See 1209.4326, also Umeh 1402.1933.

4.2. DETAILED EXPRESSION FOR $D_L(Z, \theta^A)$ 

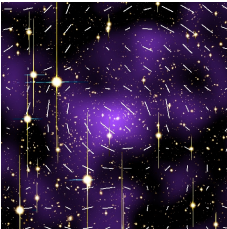
Photon enters well at a certain energy

Photon gains energy on its path into the gravitation well

Photon loses less energy than it gained on the way out of the shallower well



Gravitational well of galaxy supercluster - the depth shrinks as the universe (and cluster) expands



$$\begin{aligned}
 \delta_{\text{path}}^{(2)} = & \Xi_+ \left\{ -\frac{1}{4} (\phi_s^{(2)} - \phi_e^{(2)}) + \frac{1}{4} (\psi_s^{(2)} - \psi_e^{(2)}) + \frac{1}{2} (\psi_s - \psi_e) - \psi_s J_s^{(1)} \right. \\
 & + (\psi_s - \psi_e - J_s^{(1)}) [\partial_r Q]_* + \frac{1}{4} (\gamma_s^{\text{th}}) \partial_r Q_s \partial_r Q_e + Q_s (-[\partial_r^2 Q]_* + [\partial_r \psi]_*) + \frac{1}{\mathcal{H}_*} (\psi_s + [\partial_r Q]_*) [\partial_r \psi]_* \\
 & - \frac{1}{2} \int_{\eta_{\text{min}}}^{\eta_{\text{max}}} d\eta \frac{a(\eta)}{a(\eta_s)} \partial_r [\phi^{(2)} - \psi^{(2)}] (\eta', \Delta\eta, \hat{\theta}^a) + \frac{1}{2} \int_{\eta_{\text{min}}}^{\eta_{\text{max}}} d\eta \frac{a(\eta')}{a(\eta_s)} \partial_r [\phi^{(2)} - \psi^{(2)}] (\eta', 0, \hat{\theta}^a) \\
 & + \frac{1}{4} \int_{\eta_{\text{min}}^+}^{\eta_{\text{max}}^-} dx \partial_x [\hat{\phi}^{(2)} + \hat{\psi}^{(2)} + 4\hat{\psi} \partial_x Q + \gamma_s^{\text{th}} \partial_x Q \partial_x Q] (\eta_s^{(0)+}, x, \hat{\theta}^a) \\
 & - \frac{1}{2} \partial_x (\psi_s + \partial_r Q_s) \left(\int_{\eta_{\text{min}}^+}^{\eta_{\text{max}}^-} dx [\gamma_s^{\text{th}} \partial_x Q] (\eta_s^{(0)+}, x, \hat{\theta}^a) \right) \\
 & - \frac{1}{2} \hat{\phi}^{(2)} - \frac{1}{2} \hat{\psi}^{(2)} - K_z + \psi_s J_s^{(1)} + \frac{1}{2} (J_s^{(1)})^2 + (J_s^{(1)} - \psi_s) \frac{Q_s}{\Delta\eta} - \frac{1}{\mathcal{H}_* \Delta\eta} \left(1 - \frac{\mathcal{H}_*'}{\mathcal{H}_*^2} \right) \frac{1}{2} (\psi_s + [\partial_r Q]_*)^2 \\
 & - \frac{2}{\mathcal{H}_* \Delta\eta} \psi_s (\psi_s + [\partial_r Q]_*) + \frac{1}{2} \partial_x (\psi_s + J_s^{(1)} + \frac{Q_s}{\Delta\eta}) \left(\int_{\eta_{\text{min}}^+}^{\eta_{\text{max}}^-} dx [\gamma_s^{\text{th}} \partial_x Q] (\eta_s^{(0)+}, x, \hat{\theta}^a) \right) \\
 & + \frac{1}{4} \partial_x Q_s \partial_x \left(\int_{\eta_{\text{min}}^+}^{\eta_{\text{max}}^-} dx [\gamma_s^{\text{th}} \partial_x Q] (\eta_s^{(0)+}, x, \hat{\theta}^a) \right) \\
 & + \frac{1}{16} \partial_x \left(\int_{\eta_{\text{min}}^+}^{\eta_{\text{max}}^-} dx [\gamma_s^{\text{th}} \partial_x Q] (\eta_s^{(0)+}, x, \hat{\theta}^a) \right) \partial_x \left(\int_{\eta_{\text{min}}^+}^{\eta_{\text{max}}^-} dx [\gamma_s^{\text{th}} \partial_x Q] (\eta_s^{(0)+}, x, \hat{\theta}^a) \right) \\
 & - \frac{1}{4 \Delta\eta} \int_{\eta_{\text{min}}^+}^{\eta_{\text{max}}^-} dx [\hat{\phi}^{(2)} + \hat{\psi}^{(2)} + 4\hat{\psi} \partial_x Q + \gamma_s^{\text{th}} \partial_x Q \partial_x Q] (\eta_s^{(0)+}, x, \hat{\theta}^a) \\
 & + \frac{1}{\mathcal{H}_*} (\psi_s + [\partial_r Q]_*) \left\{ -[\partial_r \psi]_* + [\partial_r \psi]_* + \frac{1}{\Delta\eta} \int_{\eta_{\text{min}}^+}^{\eta_{\text{max}}^-} d\eta' \Delta\eta \psi (\eta', \eta_s - \eta', \hat{\theta}^a) \right\} \\
 & + Q_s \left\{ [\partial_r \psi]_* + \partial_x \left(\int_{\eta_{\text{min}}^+}^{\eta_{\text{max}}^-} dx \frac{1}{(\eta_s^{(0)+} - x)^2} \int_{\eta_{\text{min}}^+}^{\eta_{\text{max}}^-} d\eta' \Delta\eta \psi (\eta_s^{(0)+}, \eta', \hat{\theta}^a) \right) \right. \\
 & \left. + \frac{1}{2 \Delta\eta^2} \int_{\eta_{\text{min}}^+}^{\eta_{\text{max}}^-} d\eta' \Delta\eta \psi (\eta', \eta_s - \eta', \hat{\theta}^a) \right\} + \frac{1}{16 \text{stn}^2 \theta^2} \left(\int_{\eta_{\text{min}}^+}^{\eta_{\text{max}}^-} dx [\gamma_s^{\text{th}} \partial_x Q] (\eta_s^{(0)+}, x, \hat{\theta}^a) \right)^2 \quad (4.67)
 \end{aligned}$$

$$\begin{aligned}
 \delta_{\text{non}}^{(2)} = & \Xi_+ \left\{ ([\partial_r P]_* - [\partial_r P]_{s0})^2 + (\gamma_s^{\text{th}}) \partial_r P_s \partial_r P_e - \lim_{\eta \rightarrow \eta_s} [\gamma_s^{\text{th}} \partial_r P \partial_r P] \right. \\
 & - \frac{2}{\mathcal{H}_*} ([\partial_r P]_* - [\partial_r P]_{s0}) (\mathcal{H}_* [\partial_r P]_* + [\partial_r^2 P]_*) \\
 & - \int_{\eta_{\text{min}}}^{\eta_{\text{max}}} d\eta' \frac{a(\eta')}{a(\eta_s^{(0)})} \partial_r [([\partial_r P]^2 + \gamma_s^{\text{th}} \partial_r P \partial_r P)] (\eta', \Delta\eta, \hat{\theta}^a) \\
 & + \int_{\eta_{\text{min}}}^{\eta_{\text{max}}} d\eta' \frac{a(\eta')}{a(\eta_s)} \partial_r [([\partial_r P]^2 + \gamma_s^{\text{th}} \partial_r P \partial_r P)] (\eta', 0, \hat{\theta}^a) \left. - \frac{1}{2 \mathcal{H}_* \Delta\eta} \left(1 - \frac{\mathcal{H}_*'}{\mathcal{H}_*^2} \right) ([\partial_r P]_* - [\partial_r P]_{s0})^2 \right\} \quad (4.68)
 \end{aligned}$$

$$\begin{aligned}
 \delta_{\text{rand}}^{(2)} = & \Xi_+ \left\{ 2(\psi_s - \psi_e + \partial_r Q_s - \frac{Q_s}{\Delta\eta}) [\partial_r P]_{s0} - ([\partial_r P]_* - [\partial_r P]_{s0}) \left(\frac{1}{\mathcal{H}_*} [\partial_r \psi]_* - J_s^{(1)} \right) \right. \\
 & - (\gamma_s^{\text{th}}) \partial_x Q_s \partial_x P_s + \frac{1}{\mathcal{H}_*} (\psi_s + [\partial_r Q]_*) [\partial_r^2 P]_* + Q_s [\partial_r^2 P]_* \\
 & + \frac{1}{2} \partial_x ([\partial_r P]_* - [\partial_r P]_{s0}) \left(\int_{\eta_{\text{min}}^+}^{\eta_{\text{max}}^-} dx [\gamma_s^{\text{th}} \partial_x Q] (\eta_s^{(0)+}, x, \hat{\theta}^a) \right) \\
 & + \frac{1}{\Delta\eta} ([\partial_r P]_* - [\partial_r P]_{s0}) \left\{ \frac{1}{\mathcal{H}_*} \left(1 - \frac{\mathcal{H}_*'}{\mathcal{H}_*^2} \right) (\psi_s + [\partial_r Q]_*) + \frac{\psi_s}{\mathcal{H}_*} + Q_s \right\} \\
 & + \frac{1}{\mathcal{H}_*} ([\partial_r P]_* - [\partial_r P]_{s0}) \left\{ [\partial_r \psi]_* - [\partial_r \psi]_* - \frac{1}{\Delta\eta} \int_{\eta_{\text{min}}^+}^{\eta_{\text{max}}^-} d\eta' \Delta\eta \psi (\eta', \eta_s - \eta', \hat{\theta}^a) \right\} \quad (4.69)
 \end{aligned}$$

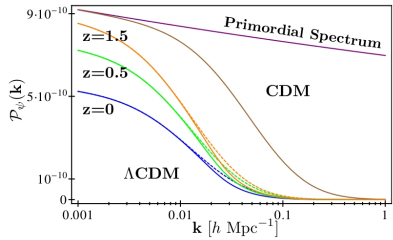
Stochastic average of inhomogeneous realizations

Inhomogeneities :

$$\psi(\eta, \vec{x}) = \int \frac{d^3k}{(2\pi)^{3/2}} e^{i\vec{k}\cdot\vec{x}} \psi_k(\eta) E(\vec{k})$$

with E a hom. and gaussian unit R.V..

Spectrum : $|\psi_k(\eta)|^2 = 2\pi^2 \mathcal{P}_\psi(k) / k^3$



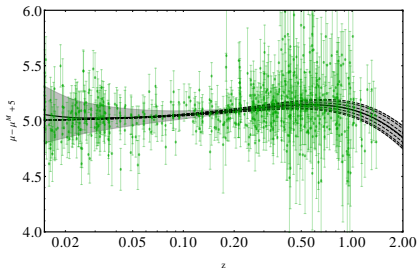
Light-cone average is combined with a stochastic average. In **CDM** :

$$\langle S \rangle_{w_o, \tau_s} = \frac{\int d^2\theta \sqrt{\gamma(w_o, \tau_s, \theta^a)} S(w_o, \tau_s, \theta^a)}{\int d^2\theta \sqrt{\gamma(w_o, \tau_s, \theta^a)}} \Rightarrow \boxed{\langle d_L \rangle = \int_0^\infty \frac{dk}{k} \mathcal{P}_\psi(k) C(k\Delta\eta)}$$

We do the same \forall terms in $\overline{\langle \delta_S^{(1)} \rangle}$ and $\overline{\langle \delta_S^{(2)} \rangle}$ in Λ CDM... with approximations.

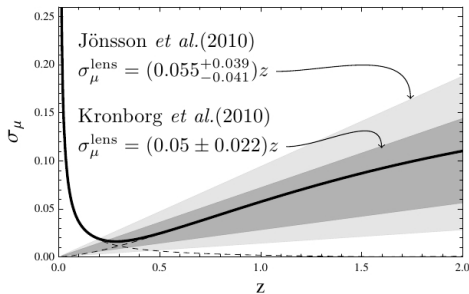
Kaiser & Peacock 2015 for precise discussion on 'directional' / 'source' averaging.

The **averaged modulus** $\overline{\langle \mu \rangle}$ depends on $\overline{\langle (d_L^{(1)}/d_L^{(0)})^2 \rangle}$ while the **standard deviation** $\sigma_\mu = \sqrt{\overline{\langle \mu^2 \rangle} - \overline{\langle \mu \rangle}^2} = 10(\log_{10} e) \sqrt{\overline{\langle (d_L^{(1)}/d_L^{(0)})^2 \rangle}}$ with

$$\overline{\langle (d_L^{(1)}/d_L^{(0)})^2 \rangle} \sim \overline{\langle (\text{Doppler})^2 \rangle} + \overline{\langle (\text{Lensing}^{(1)})^2 \rangle}$$


With the Union 2 dataset :

- small z : **Velocities** explain quite well the scatter.
- large z : **Lensing** is too weak to explain data's scatter ($\sim \% \Omega_{\Lambda 0}$).



- The total effect is well approximated by **Doppler** ($z \leq 0.2$) + **Lensing** ($z > 0.3$),
- **Lensing** prediction is in great agreement with experiments so far !

See also *Fleury, Clarkson, Maartens '17*

Other GLC applications

- Evaluate **galaxy number counts** at $\mathcal{O}(2)$ in perturbations ([Di Dio, Durrer, Marozzi, Montanari 1407.0376, 1510.04202](#)) \Rightarrow Bispectrum !
- **Inhomogeneous spacetime** : Lemaître-Tolman-Bondi with off-center observer and no curvature ([Fanizza, Nugier 2014, 1408.1604](#)), **lensing quantities** for over/under dense regions.
- Application to an **Anisotropic Bianchi I spacetime** ([Fleury, Nugier, Fanizza 2016, 1602.04461](#)). \Rightarrow we find that the **anisotropy of the Bianchi I spacetime violates** $\langle \mu^{-1} \rangle_{\Omega} = 1$!
- Application to the **time-of-flight of UR particles** ([Fanizza, Gasperini, Marozzi, Veneziano, 1512.08489](#)).
- Relation between GLC and **double-null coordinates**.
(Unrealistic) application to **static black holes** ([Nugier 2016](#)).

Number counts with GLC

Number counts of galaxies in volume $dV = (dz, d\Omega)$, defining the fluctuation $\Delta(\mathbf{n}, z) = \frac{N(\mathbf{n}, z) - \langle N \rangle(z)}{\langle N \rangle(z)}$ with $N(\mathbf{n}, z) = \rho(\mathbf{n}, z)V(\mathbf{n}, z)$ (neglecting bias), computing perturbations of density, redshift, angles, and **volume** :

$$dV \equiv \sqrt{-g}\epsilon_{\mu\nu\alpha\beta}u^\mu dx^\nu dx^\alpha dx^\beta = \sqrt{|\gamma|} \frac{\Upsilon_s^2}{\Upsilon_o \partial_\tau \Upsilon_s} dz d\theta_o d\phi_o \quad .$$

Bispectrum is given by $\langle \Delta(\mathbf{n}_1, z_1)\Delta(\mathbf{n}_2, z_2)\Delta(\mathbf{n}_3, z_3) \rangle$ at $\mathcal{O}(2)$ and the expressions can be applied to most modified gravity models. See [Di Dio, Durrer, Marozzi, Montanari, 1407.0376, 1510.04202](#). **Hundreds of terms!**

Higher-order lensing terms in **CMB lensing** can have impact on the **tensor-to-scalar ratio** of $\sim \mathcal{O}(10^{-3})$ and affect the effective number of **relativistic species** N_{eff} (see [Marozzi, Fanizza, Di Dio, Durrer '17](#)).

Also : [Biern and Yoo '17](#) compute the **luminosity distance correlation** function $\langle \delta D_L(z_1, \mathbf{n}_1)\delta D_L(z_2, \mathbf{n}_2) \rangle$.

⇒ SUB-PERCENT COSMOLOGY NEEDS THESE CORRECTIONS.

PART II

COMPARING STANDARD CANDLES AND GALAXY CATALOGUES IN OUR LOCAL UNIVERSE



Motivations

Collaboration with Hsu-Wen Chiang (蔣序文),
Enea Romano, Pisin Chen (陳丕榮).
1706.09734

- Estimate how **standard candles** can probe the **local density contrast**.
- Investigate on H_0 as *Riess 2016* re-evaluates $H_0 = 73.24 \pm 1.74 \text{ km s}^{-1} \text{ Mpc}^{-1}$, raising the **tension to 3.4σ** against $66.93 \pm 0.62 \text{ km s}^{-1} \text{ Mpc}^{-1}$ from *Planck*.
- We know that being inside an **underdensity** region may alleviate tension (see *Ben-Dayan, Durrer, Marozzi, Schwarz '14* and *Romano '16*).
- Isotropic inhomogeneity extending very far should not exist, but anisotropic inhomogeneity may. *Keenan, Barger, Cowie '13* find a **super-void** extending to $z \sim 0.07$ ($\sim 300 h_{70}^{-1} \text{ Mpc}$).

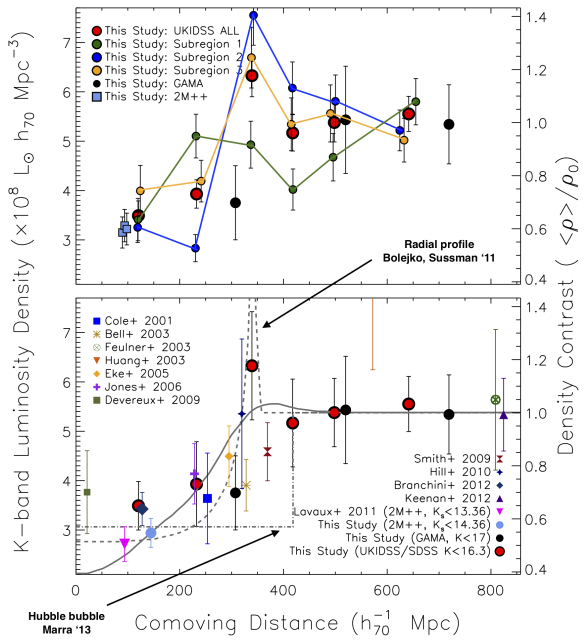
Keenan '13, Fig. 11

Comparison with density maps obtained from luminosity density of Keenan et al. 2013.

K13 uses UKIDSS, analyses K-selected catalog of 35,000 gal. ($b = 1$).

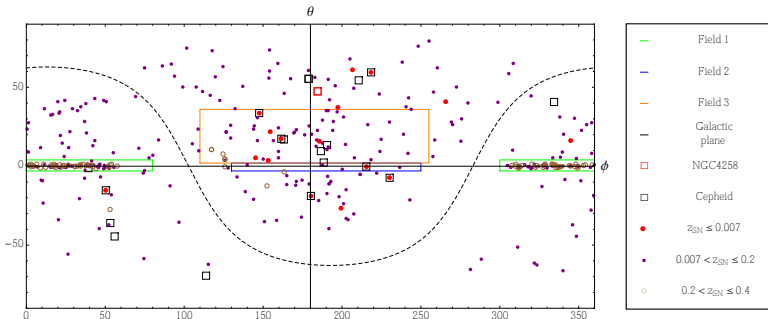
- Green : Field 1
- Blue : Field 2
- Orange : Field 3

Keenan '13 agree with 2M++ density contrast ~ 0.6 .



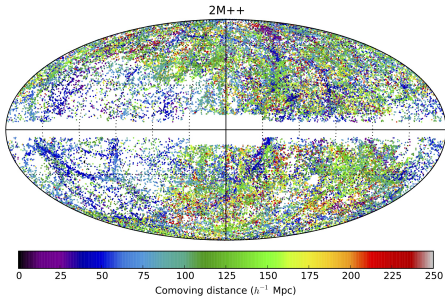
Standard Candles data

- **Cepheids** from *Riess 2016* (z_{host} from NED) and **SNe Ia** from UNION 2.1 (with z less than **0.2** or **0.4** and positions from SIMBAD).
- Use of 7 host galaxies common to $\mathcal{R}16$ Cepheids and UNION 2.1 SNe to rescale SNe Ia such that $\mu(\mathcal{R}16) = \mu(\text{Union 2.1}) - 5 \log_{10} (73.24/70)$.

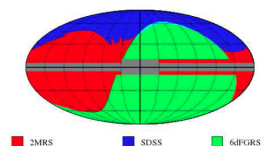


- **Velocity dispersion** : 250 km s⁻¹ for SNe, 0, 40, 250 km s⁻¹ for Cepheids. Implies a change in μ by $\Delta\mu_{\text{v.d.}} \approx \frac{5}{\log 10} \frac{\Delta v}{cz}$.

2M++ (Lavaux & Hudson 2011, Carrick *et al.* 2015)



Redshifts are from 2MRS, SDSS-DR7, and 6dFGS.

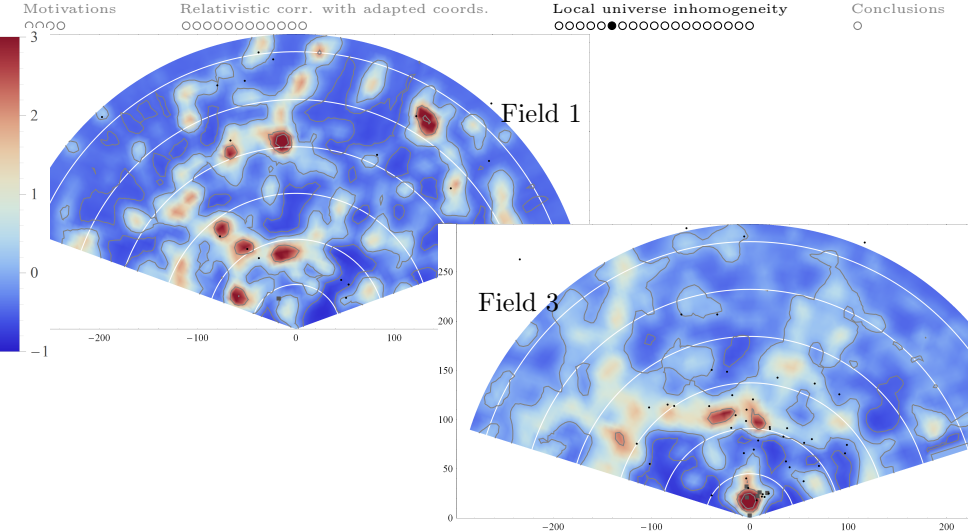


Peculiar velocity corrections (PVC) obtained from the galaxy density :

$$\vec{v}(\vec{r}) = \frac{\beta^*}{4\pi} \int_0^{R_{\max}} d^3\vec{r}' \delta_g^*(\vec{r}') \frac{\vec{r}'}{r'^3} \quad , \quad \bar{z} = z_{\text{obs}} - \vec{v} \cdot \vec{n}$$

where $\beta^* = 0.43$ is a best fit value and the upper limit of integration is the **depth of the survey** : $R_{\max} = 200 h^{-1} \text{Mpc}$, i.e. $z = 0.067$.

\Rightarrow limited to **200 $h^{-1} \text{Mpc}$ + an external bulk flow** (that we remove).



Comparison with 2M++ density map (averaged along declination direction in ICRS coordinates).

White arcs correspond to $z = 0.01, 0.02, \dots, 0.06$, gray contours indicate iso-density lines of $\delta_C = -0.5, 0, 2, 4$.

1D Fitting

Fits of the distance modulus data $(z_i, \mu_i, \Delta\mu_i)$ by minimizing χ^2 of the deviation from a homogeneous model :

$$\chi^2 = \sum_i \left(\frac{f(z_i) - (\mu_i - \mu^{\text{Planck}}(z_i))}{\Delta\mu_i} \right)^2, \quad f(z) = (\mu^{\text{obs}} - \mu^{\text{Planck}})(z)$$

where $\mu^{\text{Planck}}(z)$ is the Λ CDM theoretical value of distance modulus at z .

Model independent by decomposing the fitting function $f(z)$ wrt a set of *radial basis functions* (RBFs NN) :

$$f(z) = w_0 + w_{-1} z + \sum_{m=1}^{N_{\text{NL}}} w_m \Phi(|z - p_m|)$$

where Φ are chosen to be $\Phi(r) = r^3$ (N_{NL} RBFs), p_m are the **non-linear parameters** or “centers” of the RBFs, w_m the linear parameters, w_0 (intercept) and/or w_{-1} (slope) parameters.

Best fit and confidence bands

- **Linear parameters** $\mathbf{w} \equiv (w_{-1}, \dots, w_{N_{\text{NL}}})$: we use the simple Moore-Penrose pseudo-inverse method.
- **Non-linear parameters** $\mathbf{p} \equiv (p_1, \dots, p_{N_{\text{NL}}})$: we use a Monte Carlo (MC) random sampling method and a LO algorithm (Gauss-Newton).
- **To speed up the MC process and fill up confidence band** we use a MCMC algorithm to explore the non-linear parameter space.

A **fitting model** is classified by a set of parameters $(N_0, N_{-1}, N_{\text{NL}})$.

We use a F-test to determine the **best model parameters**.

+ **Inversion** in each field based on Lemaître-Tolman-Bondi (LTB) in 1D (neglecting transverse shear) to reconstruct the local radial density profile (assuming Planck background). See [Romano, Chiang and Chen, 2013](#).

⇒ **Density contrast** :

$$\delta_C = \Omega_{m0}^{-0.55} \left(\frac{\rho_{\text{inv}}(D_L, z)}{\rho_{\text{inv}}(D_L^{\text{Planck}}, z)} - 1 \right) .$$

Full sky fitting

Applying PVC from 2M++ and velocity dispersion (VD) of 250 km s⁻¹ for SNe.

VD = 250 km s⁻¹ for Cepheids (like Riess 2016) :

⇒ Preferred model is (1,0,0) : $f(z) = w_0$, i.e. homogeneous with :

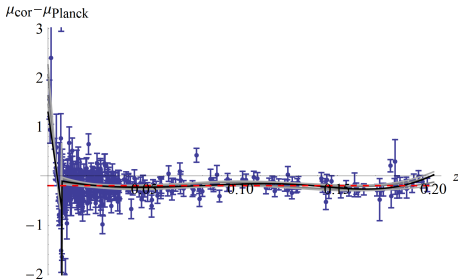
$$H_0^{\text{loc}} \equiv H_0^{\text{Planck}} 10^{-f(z=0)/5} = H_0^{\text{Planck}} 10^{-w_0/5} = 10^{-w_0/5} (66.93 \text{ km s}^{-1} \text{ Mpc}^{-1}).$$

We find : $H_0^{\text{loc}} = 73.06 \pm 1.61$ (stat.) km s⁻¹ Mpc⁻¹, in good agreement with 73.24 ± 1.61 (stat.) ± 0.66 (sys.) km s⁻¹ Mpc⁻¹ of Riess 2016 (we have $\chi_R^2 = 1.49$).

VD = 40 km s⁻¹ for Cepheids :
(see Tully 2007)

Best fit is a (0, 1, 7) model!
 $\chi_R^2 = 4.18$

⇒ there seems to be structure not accounted for by 2M++.

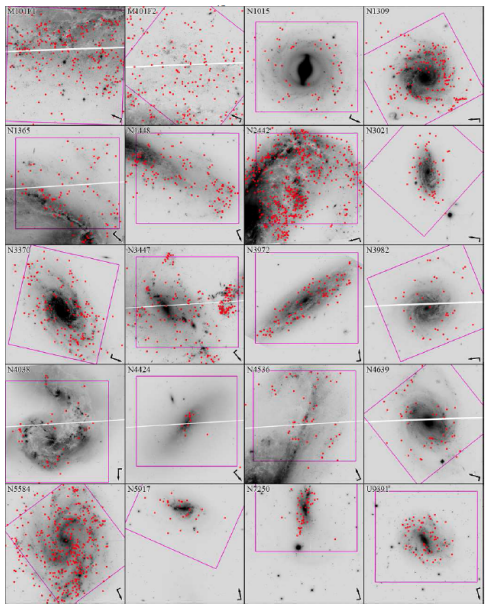


Cepheid hosts

We decide to give more importance to the Cepheid hosts and assume :
 $VD = 0 \text{ km s}^{-1}$.

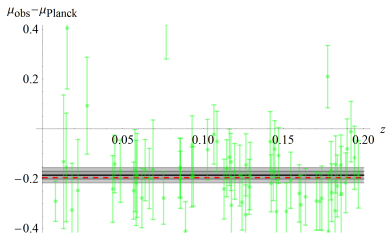
Could NGC 4536 be biased ?

See [Hoffmann '16](#) for more information about Cepheids.

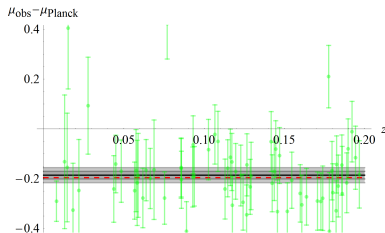


Directional fitting in F1

With PVC from 2M++ :



Without PVC from 2M++ :



- **best fit** we get is a **(1,0,0)** model with $H_0^{\text{loc}} = 72.89 \pm 0.50 \text{ km s}^{-1} \text{ Mpc}^{-1}$ and $\chi_R^2 = 1.05$,
- next best fit (Threshold < 33%) is given by a (0, 1, 5) model with $\chi_R^2 = 0.88$.

- **best fit model is (1,0,0)** with $H_0^{\text{loc}} = 72.90 \pm 0.51 \text{ km s}^{-1} \text{ Mpc}^{-1}$ with F-test *Threshold* > 36% and $\chi_R^2 \sim 1.07$,
- second best model is an inhomogeneous (1, 1, 13) model with $\chi_R^2 \sim 0.59$ but low threshold.

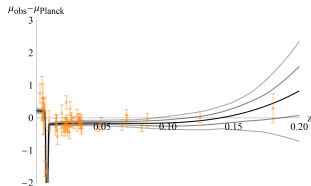
Directional fitting in F3 with PVC

Applying PVC from 2M++ and VD of 250 km s^{-1} for SNe Ia (host rotation) and no VD for Cepheids.

Use a F-test *Threshold* $\sim 95\%$ to compare models.

$z_{\max} = 0.2$			
χ_R^2	Threshold (%)	Param.	Removal
19.5	Not Preferred	76.40 ± 2.90	
1.59	81 \sim 100	(0, 1, 6)	
5.92	95.8 \sim 100	(0, 0, 0)	NGC 4536
2.06	90.7 \sim 95.7	(0, 1, 3)	Same
2.05	73 \sim 100	70.56 ± 0.93	+NGC 4424

$z_{\max} = 0.4$			
χ_R^2	Threshold (%)	Param.	Removal
17.9	Not Preferred	76.36 ± 2.75	
1.60	74 \sim 100	(0, 1, 6)	
5.58	96.9 \sim 100	(0, 0, 0)	NGC 4536
2.03	85 \sim 96.8	(0, 1, 3)	Same
2.00	72 \sim 100	70.65 ± 0.91	+NGC 4424



Based on no-PVC (but similar)

\Rightarrow Necessary to remove some “outliers” to have invertible fits!

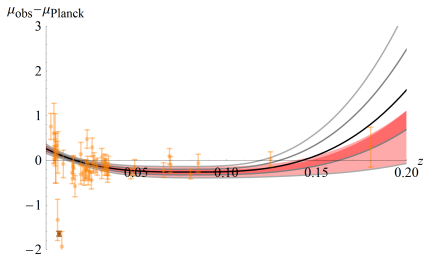
Directional fitting in F3 without PVC

We don't apply PVC since we want to see the whole contribution from SNe Ia and Cepheids.

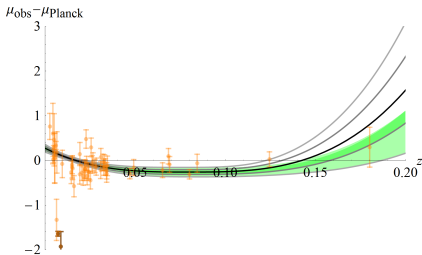
Just apply a VD of 250 km s^{-1} for SNe Ia (host rotation).

$z_{\max} = 0.2$			
χ_R^2	Threshold (%)	Param.	Removal
1.40	39 ~ 100	(0, 0, 5)	
3.45	97.5 ~ 100	(0, 0, 0)	NGC 4536
2.26	89 ~ 97.4	(1, 0, 1)	Same
2.88	99.5 ~ 100	(0, 0, 0)	+1999cl
1.55	94.1 ~ 99.4	(1, 0, 1)	Same
1.47	47 ~ 94.0	(0, 0, 2)	Same

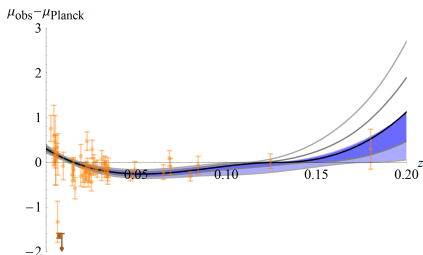
$z_{\max} = 0.4$			
χ_R^2	Threshold (%)	Param.	Removal
1.43	38 ~ 100	(0, 1, 5)	
3.31	92.6 ~ 100	(0, 0, 0)	NGC 4536
2.20	92.1 ~ 92.5	(0, 1, 2)	Same
2.80	96.3 ~ 100	(0, 0, 0)	+1999cl
1.96	89 ~ 96.2	(1, 0, 1)	Same
1.37	76 ~ 88	(0, 0, 4)	Same



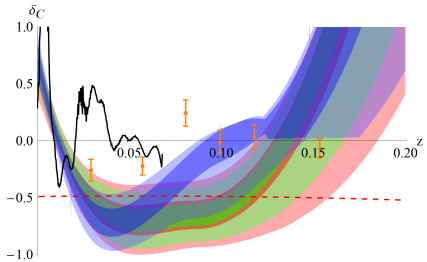
(a) NGC 4536 removed (1, 0, 1)



(b) NGC 4536, 1999cl removed (1, 0, 1)

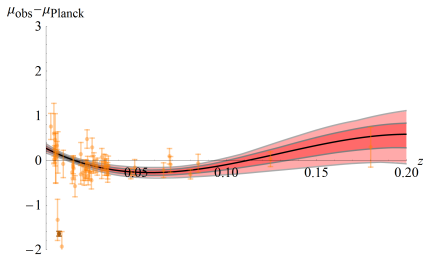


(c) NGC 4536, 1999cl removed (0, 0, 2)

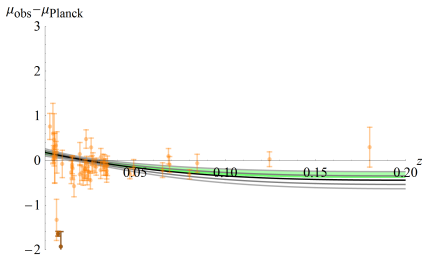


(d) Inverted density

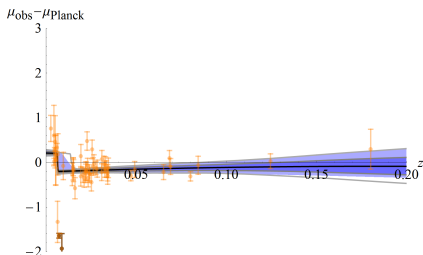
FIGURE: Distance modulus best fit models are plotted for F3 with $z_{\max} = 0.2$, without peculiar velocity corrections and with a 250 km s^{-1} velocity dispersion for SNe.



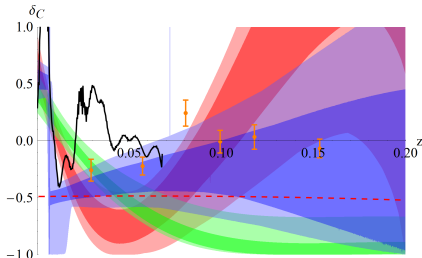
(a) NGC 4536 removed (0, 1, 2)



(b) NGC 4536, 1999cl removed (1, 0, 1)



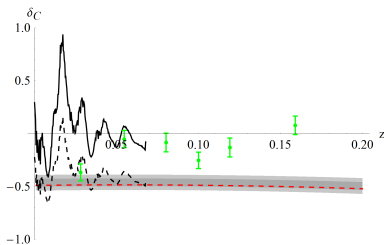
(c) NGC 4536, 1999cl removed (0, 0, 4)



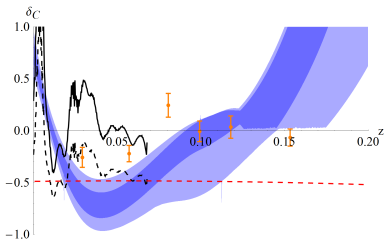
(d) Inverted density

FIGURE: Distance modulus best fit models are plotted for F3 with $z_{\max} = 0.4$, without peculiar velocity corrections and with a 250 km s^{-1} velocity dispersion for SNe.

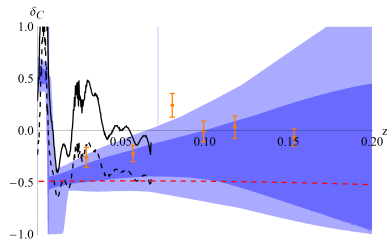
Main results



(a) Field 1, (1, 0, 0)



(b) Field 3, $z_{\max} = 0.2$ with NGC 4536 and 1999cl removed (0, 0, 2)



(c) Field 3, $z_{\max} = 0.4$ with NGC 4536 and 1999cl removed (0, 0, 4)

Rescaling $2M_{++}$

- $2M_{++}$ is normalized wrt the average within its depth \Rightarrow its normalization can be wrong if $2M_{++}$ is embedded in a larger structure.
- Same with [Keenan 2013](#) with background equal to the averaged luminosity density over the data set.
- **Our reconstructed density profile is normalized wrt the background** since we are assuming cosmological background parameters obtained from large scale observations (Planck).

If we take $\mathcal{K}13$ background density we would have to rescale $2M_{++}$ as

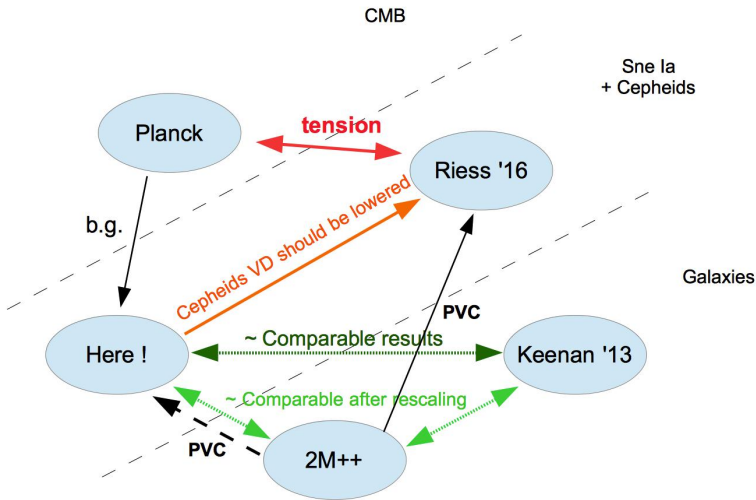
$$\delta_C^{\text{cor}} = \frac{\tilde{\rho}_{2M_{++}}}{\tilde{\rho}_{\mathcal{K}13}} (1 + \delta_C) - 1,$$

where δ_C^{cor} is the rescaled density contrast, while $\tilde{\rho}_{2M_{++}}$ and $\tilde{\rho}_{\mathcal{K}13}$ are the assumed background density of $2M_{++}$ and $\mathcal{K}13 \Rightarrow$ **factor 0.6 rescaling**.

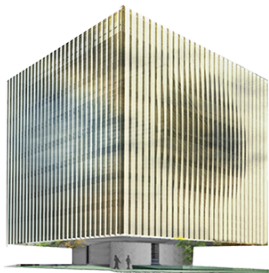
Summary

- SNe + Cepheids hosts appear to independently confirm the existence of **inhomogeneities**,
- to some extent in qualitative agreement with Keenan 2013 (claiming ~ 300 Mpc void), but **normalization of background seems crucial**,
- based on **1D fit** in windows of the sky, **LTB inversion** model, with SNe Ia and Cepheids data \Rightarrow different sources of uncertainty,
- SNe Ia could be useful to **correctly normalize density maps** from galaxy surveys with respect to the average density of the Universe,
- **could clarify apparent tension** between local and large scale estimations of H_0 (especially between Planck and Riess which uses $2M++$).

Summary picture



どうもありがとうございます。



LeCosPA @ NTU has new building, please come give a seminar! :-)

I) The **large scale structure** sources **relativistic corrections** to all cosmological observables, important for **percent accuracy** in cosmology.

Adapted coordinates are useful!

II) The **local structure** needs careful studying, with precise data. It may contain the solution of the **critical H_0 tension!**

Thank You!